Climatology of ionosphere over Nepal based on GPS TEC data from 2008 to 2018

Drabindra Pandit[1, 6],Basudev Ghimire[1,6], Christine Amory-Mazaudier[2, 3], Rolland Fleury[4], Narayan Prasad Chapagain[5], Binod Adhikari[6]

1. Central Department of Physics, IOST, Tribhuvan University, Kathmandu, Nepal
2. Sorbonne Universités UPMC Paris 06, LPP, Polytechnique, France
3. T/ICT4D Abdus Salam ICTP, Italy
4. Lab-STICC, UMR 6285, Institut Mines-Telecom Atlantique, site de Brest, France
5. Amrit Campus, Tribhuvan University, Thamel, Kathmandu, Nepal
6. Department of Physics, St. Xavier's College, Maitighar, Kathmandu, Nepal

Abstract

In this study, we analyze the climatology of ionosphere over Nepal based on GPS derived VTEC observed from four stations: KKN4 (27.80° N, 85.27° E), GRHI (27.95° N, 82.49° E), JMSM (28.80° N, 83.74° E), DLPA (28.98° N, 82.81° E) during years 2008 to 2018. The study illustrates the diurnal, monthly, annual, seasonal and solar cycle variations of VTEC during all time of solar cycle 24. The results clearly reveal the presence of equinoctial asymmetry in TEC which is more pronounced in maximum phases of solar cycle in year 2014 at KKN4 station followed by descending, ascending and minimum phases. Diurnal variation of VTEC showed short-lived day minimum which occurs between 5:00 to 6:00 LT at all the stations considered with diurnal peak between around 12:00 to 15:00 LT. The maximum value of TEC is observed during spring equinox than autumn equinox with a few asymmetries ~~anomalies~~. Seasonal variation in TEC is observed to be a manifestation of variation of solar flux, particularly the level of solar flux in consecutive solstices. ~~Similarly, winter anomalies are noticed during increasing and maximum phases of the solar cycle 2011 and 2014 from almost all stations taken in the study.~~

1. Introduction

Total electron content (TEC) is a crucial parameter of ionosphere comprising high concentration of electrons and ions, formed under the ionization of extreme ultraviolet (EUV) radiation and solar X-rays. The lower atmospheric disturbance also contributes to ionospheric variability

(Anderson and Fuller-Rowell, 1999; Prikryal et al., 2010). A numerous periodic and aperiodic variability identified in the ionosphere makes impact on the applications involving radio link between satellites and ground which play vital role in the communication, navigation and surveillance with important consequences for the reliability and accuracy of the service (Guo et al., 2015). Global positioning system (GPS) is widely used in recent appliances which encounter largest errors in the path due to disturbed ionospheric free electrons which emphasizes to study GPS-TEC variability. The application of GPS technology allows scientists insight into the shape and behavior of ionosphere. List of factors affecting TEC are ionospheric electron density, ion-electron temperature, composition, dynamic vary with altitude, latitude, longitude, local time, seasons, solar as well as magnetic activity. Equatorial ionosphere is being highly vulnerable possess major threats to the communication signals. The ionosphere at mid latitude is less variable hence ~~the~~ most of the observations and measurements are taken from this region where as high latitude ionosphere is sensitive to outer space connected by geomagnetic field lines (Akala et al.,2013;Parwani et al., 2019). Study of VTEC at low-mid ionosphere showed solar activity dependence (Shimeis et al., 2014). TEC has been studied by large number of researchers, Rama Rao et al. (1980) studied the diurnal variation in TEC at Waltair, India and found short lived pre-dawn minimum, a steep early morning rise followed by broad mid afternoon maximum and a steep post sunset fall. The relation between TEC and SSN, $F_{10.7}$and EUV was studied by Dabaset al. (1993) and pointed out that TEC has nonlinear relation with SSN and linear relation with $F_{10.7}$ and EUV. Ouattara and Amory- Mazaudier (2012) showed impact of solar activity on diurnal variability during different phases of solar cycle. Analogous study was carried around the globe using various methods on TEC such as diurnal, monthly, seasonal and solar cycle and solar activity dependency e.g. in South Asia (Chauhan et al., 2011; Walker et al., 1994); in South America (Sahai et al., 2007; Natali and Meza, 2011; Akala et al., 2013; de Abreu et al., 2014); over North America (Huo et al., 2009; Perevalova et al., 2010); in Africa (Shimeis et al, 2014; D'ujanga et al., 2012; Ouattara and Fleury, 2011; Zoundi et al., 2012); over Brazil (Venkatesh et al., 2014a, 2014b, 2015) ; over Japan (Zakharenkova et al., 2012; Mansoori et al., 2016); over China (Guo et al., 2015; Zhao et al., 2007 ; Liu et al., 2013).

TEC studied at Jet Propulsion laboratory for the year (1998-2008) found stronger annual TEC variation in southern hemisphere and variation in phase and amplitude is more in conjugate hemisphere (Liu et al., 2009). Galav et al. (2010) found semiannual periodicity in daytime TEC, and the spring equinox shows highest TEC and winter solstices the lowest in India. The winter anomaly, semiannual anomaly and annual anomaly are described in paper by Liu and Chen (2009); Rishbeth and Garriott (1998). Global scale TEC research found that the effect on TEC was stronger on day than at night and also at low latitude than in high latitudes. The effect on TEC is seen more on the either side of dip equator than at dip equator (Liu et al., 2009). Dashora and Suresh (2015) analyzed the characteristics of low latitude TEC data of solar cycle 23 and 24 over Indian sector using global ionospheric data. A double hump structure in solar flux as well as in TEC was identified at low latitude station Varanasi, India in ionospheric response using GPS TEC, IRI and TIE-GCM TEC of solar cycle 24 by Rao et al., (2019a). Parwani et al. (2019) studied latitudinal variation of ionospheric TEC at northern hemispheric region and found that the diurnal TEC has higher value in low than in mid and high latitude and in seasonal variation maximum in Spring and autumn than in summer and winter.

Many studies on TEC have been conducted in Asia, however no result for the climatology of TEC over Nepal for a long-time series, about one solar cycle has been reported up to now. In this paper, we present for the first-time characteristics of ionosphere in Nepal such as the diurnal, annual, seasonal and solar cycle dependence of TEC on the local ionospheric conditions using GPS TEC data obtained from four GPS stations: KKN4, GRHI, JMSM and DLPA. Our study includes GPS TEC data from 2008 to 2018 of the solar cycle 24, including all four phases of this solar cycle, the minimum phase of year 2008-2009; ascending phase of year 2010-2013, maximum phase of year 2014 and descending phase of year 2015-2018. The second section of this paper includes the dataset and methodology, the third for the results and discussion. The concluding remark is discussed in the last section.

2. Dataset ~~Data sets and data analysis~~

Total electron content (TEC) is total number of electrons integrated along the path from receiver to each GPS satellites which orbits the Earth at altitude of 20,200 km. It measures in TECU, 1TECU = 10^{16} electron/m^2. The TEC is obtained as (Hofmann-Wellenhof et al., 1992)

$$\text{TEC} = \int_R^S N_e\,(h)dh \qquad (1)$$

Where, N_e is electron density, R is the receiver altitude and S the satellite altitude. The dual frequency GPS receiver in two L-band of frequency: f_1 = 1575.42 MHz and f_2 = 1227.60 MHz provide the carrier phase and pseudo-range measurements. The TEC is calculated from these L1 and L2 pseudo-range and carrier phase (Hofmann-Wellenhof et al., 1992). Using pseudo-range and phase data, TEC is calculated as

$$\text{TEC} = \frac{1}{40.3}\left(\frac{{f_1}^2\,{f_2}^2}{{f_2}^2 - {f_1}^2}\right)(P_1 - P_2) \qquad (2)$$

Where, P_1 and P_2 are the pseudo-ranges for frequencies f_1 and f_2, respectively.

The TEC obtained by this method is called slanted TEC (STEC) which is a measure of the total electron content of ionosphere along the ray path from the satellite to receiver has to be converted to vertical TEC (VTEC) using equation (Titheridge, 1972).

$$\text{VTEC} = (\text{STEC} - B_s - B_u)\left(\sqrt{1 - \left(\frac{(R_e \times cos\varepsilon)^2}{(R_e + h)^2}\right)}\right) \qquad (3)$$

B_s and B_u are the biases of instruments of satellites and receivers respectively, ε is the elevation angle of satellite and R_e = 6371 km is the mean radius of the Earth.

For this study data was carried out with GPS data taken from four GPS stations: DLPA, JMSM, KKN4 and GRHI from Nepal. The details of the stations including their geographical and geomagnetic coordinates are shown in table 1 and Universal time is considered as all-time references. The GPS data of the four stations were downloaded from www.unavco.org which is freely available to all users. This data is available in RINEX (Receiver Independent Exchange format) v2.1 which is a standard ASCII format. The temporal resolution of this data is 15 min. The raw data is then processed using software developed by Rolland Fleury (Rolland Fleury, July 19, 2018, on the website www.girgea.org) from Lab-STICC, UMR 6285, Institut Mines-Telecom Atlantique, site de Brest, France which runs on a window operating system to get required TEC.

The data for solar indices sunspot number (SSN) and solar flux index (F10.7) to study long term solar activity are taken from Royal Observatory of Belgium, Brussels, through website: sidc.oma.be/silso/home and OMNI website http://omniweb.gsfc.nasa.gov/.SSN is most consistent solar indices effectively describes solar activities and are valuable mode in forecasting space weather phenomena. The solar flux index provides the information about the total emission produced by the Sun at the wavelength of F10.7 cm at the Earth.

In this study, we use GPS derived TEC from RINEX file using this method to obtain TEC calibrated at 15 minutes for all measures. Between 30s VTEC sequences, the elevation may vary. This leads to variation in the VTEC depending on the constellation and not just the variation of the content over that period. We have chosen to do the regression over a period 15 minutes with the VTEC obtained displayed in the middle of this period. This makes it possible to have 4 points over 1 hour and therefore to have an evolution of the VTEC 4 times more precise than that of GIM maps which are currently in steps 1 or 2 hours depending on the organization. So, it is better possibility to see and characterize finer local structures in RINEX derived TEC than in GIM.

This study analyzes variations of VTEC during different phases of solar cycle 24 along with annual, seasonal and diurnal variation. For this local season classified as winter (November, December, January and February), spring (March and April), summer (May, June, July and August) and autumn (September and October). The classifications of selected years as per solar cycle phases are presented in table 2.

3. Results and Discussion

In this section, we present the diurnal, monthly, seasonal, solar cycle and geomagnetic variation in GPS TEC over Nepal during the solar cycle-24. Figure 1 represents the position of chosen GPS stations in Nepal for this study and Figure 2 represents the variation of sunspot number and solar flux during the period 2008-2018. ~~In this section, we present the signatures of diurnal, monthly, seasonal, solar cycle and geomagnetic variation on GPS VTEC over Nepal which is calculated using Rolland software (as described in sec. 2). Figure 1 represents the position of GPSTEC stations in Nepal used for this study and Figure 2 represents the variation of sunspot number and solar flux for the year 2008 to 2018~~.

3.1 Diurnal variation

Figure 3a exemplify diurnal variation of VTEC in LT time observed during February 2, 2009, 2012, 2014, 2016 and 2017during the minimum, inclining increasing, maximum and declining decreasing phases of solar cycle 24 at KKN4 station in Nepal. The plot shows before sunrise ~5:00 LT, VTEC becomes minimum and reaches a maximum around 11:00-14: 00 LT and later decreases in the evening and night. The diurnal peak is noticed between 11:00 to 14:00 LT though the peak values change every month. The VTEC plots reveal a growth from dawn to a highest value about 5 to 98 TECU after the hours of daylight, it decreases to the lowest value prior to dusk with time difference of ±1 to 2 hours. A flat curve with minor peaks is identified during minimum and descending phases whereas dome shape is noticed during maximum phase, multiple peaks and trough at varying position is observed during ascending phases. In overall, the VTEC shows a normal trend of diurnal behavior with the lowest value in dawn and dusk and the highest value during the midday. The maximum VTEC in diurnal curve noticed during maximum phases of the solar cycle 2014 then in 2012 the ascending phases and minimum in 2016, 2017 and 2009 during descending and minimum phases. Diurnal variation of VTEC was studied by plotting similar curves for all the days from year 2008 to 2018 for all chosen four stations. Diurnal variation of VTEC was studied by plotting similar curves for all the days from year 2008 to 2018 for all chosen four stations. In general, the diurnal VTEC behavior exhibits the solar cycle dependency. The diurnal variability of VTEC for all the day is not presented due to constraint of space. In our study the mean diurnal curves for KKN4 station of years 2008, 2009 and 2010 exhibits wave like profile whereas the mean diurnal curves of years 2011, 2012, 2013, 2014, 2015, 2016 and 2017 show parabolic nature which is shown in Figure 3b. The similar diurnal profile was noticed for all the stations considered. The diurnal graphs (Figure 3) show better synchronization of VTEC with SSN and solar flux (Figure 2).

The observed diurnal VTEC pattern reflects the different solar events signature. The noon bite out profile with asymmetric peaks, parabolic profile and wave profile with morning, evening and night peaks and few complex structures are noted in diurnal profile. The quiet day activity at minimum phase, the fluctuating activity during increasing phase, shock activity during maximum phase and recurrent activity during declining phase was noticed in the study of ionospheric parameters at Ouagadougou ionosonde station data in West Africa by Ouattara et al. (2009).

The upward $\vec{E} \times \vec{B}$ drift velocity plays an important role in producing the nighttime post sunset enhancement. The average plasma flux required for the enhancement in equatorial latitude found

(2.2 ±0.9) x10^{12} $m^{-2}s^{-1}$ by Jain (1987) in India. In 2015 Tariku, studied pattern of GPS-TEC over African sector during 2008 to 2009 and 2012 to 2013 and found small enhancements in the VTEC in the nighttime ~ between 21:00 to 23:00 LT especially for equinoctial months and then drops again mostly after 23:00 LT. The enhancement was mostly found in equinoctial months during high solar activities and during low solar activities phase in solstice the pre-reversal enhancement was much smaller. A diurnal plot (Figure 3) of ionosphere over Nepal shows similar result of pre-reversal enhancement during high solar activities 2012 and 2014 but not during low solar activities of 2009 and2017.

Mountains generate relief waves which propagate to stratosphere and lower thermosphere (Martin Leutbecher and Hans Volkert, 2000). Studies on these waves have been made in Nepal in the lower atmosphere (Regmi, R.P. and S. Maharjan, 2015; Regmi et al., 2017). Other studies have shown the impact of relief waves on the ionosphere in the Andes (Torre et al., 2014) and Tibet (Khan A., S. Jin, 2018). In the figure 3a we see oscillations which cannot be interpreted directly as the signature of the waves. In fact, for the processing of GPS data, we use pseudo-range signals which can be affected by reflections on surrounding reliefs as well as by waves.

3.2 Monthly variation in TEC

Figure 4 shows the monthly variability of VTEC for the maximum phase of solar cycle year 2014 at KKN4 station. The plot is obtained using average of daily data. The plot shows maximum in equinoctials months (March, April) and minimum in solstices (January, June). The rise or fall of TEC in each curve follows the diurnal pattern, prominent peak in the midday with different peak amplitude. The lowest VTEC peak observed during January and highest in March. Late afternoon peak noticed in March, June and September whereas the peak centered ~ 2:00 LT for rest of the months. A significant plat peak noticed in December whereas the steep rise in VTEC is noticed in March, April and October. Monthly variation of VTEC was studied by plotting similar curves for all the month from year 2008 to 2018 for all chosen four stations. The plot shows clear wave's activity in mean diurnal curve for year 2008, 2009 and 2010 and from the years 2011 to 2017 the stiff rise in VTEC was noticed ~~and in 2017 the wave activity starts again~~ (plots are not included in this paper). In general, the sunrise time in summer and winter is 5:15 LT and 6:45 LT which are differ by 1.5 hours. During summer 2014, the maximum and minimum TEC observed is 21 and 12 TECU ~~tecu~~ whereas in winter the maximum and minimum

TEC noticed is 25 and 15 TECU ~~tecu~~ respectively (Figure 4). It also seems that during sunrise time in summer the VTEC is linear but during the winter it is steep.

3.3. Seasonal variation in TEC

Figures 5 show two dimensional diurnal plot of VTEC at JMSM station for all the four phases (I minimum-2009, II ascending-2011, III maximum-2014 and IV descending-2015) of the solar cycle 24 which explains how diurnal VTEC varies hourly during four phases. In ionosphere over Nepal the features of equinoctial asymmetry is distinctly noticed in 2D plots of year 2009, 2011, 2014 and 2015 in Figure 5a, 5b, 5c and 5d, respectively. From Figure 5a, 5b, 5c and 5d it is observed that equinoctial asymmetry is not noticed in 2009, in 2011 autumn is more intense than spring and in 2014 and 2015 spring VTEC is greater than autumn. In year 2009, equinoctial asymmetry is not noticed during low solar activities. But in year 2011, the autumn is intense than spring which is the features of equatorial ionization anomaly (EIA) crest latitude and in year 2014 the difference between equinoctial asymmetry is less (spring > autumn) which is again the characteristics of the EIA trough station. And in 2015, the asymmetry very high (spring > autumn) which is the general feature of TEC at all latitude. ~~Our study can conclude that ionosphere Nepal sometimes show features of EIA crest latitude and sometimes EIA trough station.~~

In the Figures 6a, 6b, 6c, 6d and 6e each panel separately represents the VTEC variation during autumn, spring, summer and winter season for the year 2008, 2009, 2011, 2014 and 2015 at KKN4, GRHI, JMSM and DLPA respectively. The plots show the maximum values of VTEC is ~95 TECU ~~tecu~~ in spring 2014 the maximum year of sunspot cycle and minimum value 10 TECU ~~tecu~~ in 2009 winter the minimum year of sunspot cycle. In the increasing and decreasing phases of solar cycle, the VTEC gradually increases and decreases depending to the amount of UV that arrive the Earth. In general, the plots show that VTEC is maximum during spring followed by autumn, summer and winter, except few cases. Similarly, previous study of GPS TEC for the year 2014 over Nepal also reported the highest value of VTEC on March and lowest on December with distinct the seasonal variations having higher values in spring and lower in winter season (Ghimire et al., 2020). During the sunspot minimum years 2008 and 2009 and 2010, there are no semi-annual variations in the VTEC and it also seems the summer VTEC is as strong as the Autumn VTEC. For the years 2011 to 2016 the semi-annual variations are noticed.

During the year 2017, we observed the same pattern as for the year 2008, 2009 and 2010, the summer VTEC is as strong as the Autumn VTEC. At the station KKN4, the VTEC in autumn is very weak in year 2015 and it is smaller than the VTEC in summer. In year 2011 ~~winter anomaly is noticed~~ the VTEC is larger in Winter than in Summer at KKN4 whereas GRHI and JMSM the Winter VTEC is ~~observed~~ smaller than the Summer one in year 2011 and 2014. ~~Winter anomaly is not observed~~ At DLPA, the Winter VTEC is not larger than the Summer VTEC. In year 2008 spring VTEC identified more than autumn for GRHI, JMSM and DLPA but less than autumn is observed KKN4. In year 2009 only at JMSM spring noticed greater than autumn. The autumn VTEC is greater than spring for all station in 2011 except at JMSM it equal to spring. Large asymmetry is noticed between spring and autumn in year 2014. In year 2015 the summer peak is higher than autumn. In present study the VTEC larger in winter than VTEC in Summer ~~winter anomaly~~ is noticed in 2011 and 2014. At KKN4 station the VTEC larger in winter than VTEC in Summer ~~winter anomaly~~ is noticed in the year 2014; at GRHI 2014 and 2016; at JMSM 2014 and 2016. The VTEC larger in winter than Summer VTEC ~~Winter anomaly~~ is not noticed at DLPA (Figure 6c and 6d).

Solar flux dependency of winter anomaly in GPS TEC has studied by Rao et al. (2019b). The result showed that when the level of solar flux in winter month is greater than the corresponding summer month winter anomaly is observed irrespective to the phases of solar cycle whether it is high or low. Their study also pointed out that the winter anomaly in GPS-derived TEC may not be a feature of any geophysical significance. The winter or seasonal anomaly introduced due to temperature changes (Appleton, 1935), inter hemispheric transport of ionization (Rothwell, 1963), the significant changes in the Sun-Earth distance (Yonezawa, 1959), seasonal variation of O/N2 concentration (Rishbeth and Setty, 1961; Wright, 1963; Rishbeth et al., 2000; Zhang et al., 2005) and the upward movement of energy flux (Maeda et al., 1986). The winter anomaly is related to solar activity. Tyagi and Das Gupta (1990) and Bagiya et al (2006) have reported absence of winter anomaly in low solar activities at low latitudes. The change in composition of the constituents being identified as cause of the winter anomaly is coined by Rishbeth and Setty (1961).The least VTEC in June solstice (in Northern hemisphere) during the low and high solar activity phase may be due to the asymmetry heating and which result in transport of neutral constituents from summer to winter hemisphere reducing the rate of recombination. The reduction in recombination rate in winter causes the rise of VTEC in winter than in summer.

Gupta and Singh (2001) studied TEC over Delhi and concluded that winter anomaly in TEC appears only during higher solar activity. This winter anomaly is due to the closer distance of the Earth from the Sun and the direction of the wind from the summer season to the winter (Shimeis et al, 2014). Krankowsky et al. (1968) and Cox and Evans (1970) separately pointed out that the ratio of O/N_2 become twice in winter than in summer as a result of higher electron loss rate in summer than in winter. Torr and Torr (1973) observed the winter anomaly in foF_2 under different solar activity at the mid latitude of northern hemisphere and similar result was observed in southern hemisphere during high solar activity. Furthermore, they noticed lower solar activities results lower winter anomaly. In general, June solstice anomaly is higher than the December solstice but in earlier, study done at Agra GPS station noticed some abnormalities in the solstice behavior demonstrating higher VTEC in the summer than autumn and winter anomaly with higher VTEC than in summer (Bagiya et al., 2011).

In Figure 7 top left panel represents the variation of VTEC during spring, down left during autumn, top right during summer and bottom right during winter from year 2008 to 2017 at KKN4. In spring the difference in VTEC between high and low solar activity is 65 TECU ~~tecu~~, in autumn 53 TECU ~~tecu~~, in summer 45 TECU ~~tecu~~ and in winter 40 TECU ~~tecu~~ respectively. In Figure 8 the top panel represents VTEC variability during minimum and increasing phases whereas the bottom panel represents the maximum and decreasing phases of solar cycle 24 using GPS station at GRHI. The plot shows that equinoctial asymmetry is not observable during minimum solar cycle 2008 and 2009, it is clearly distinguishable during other phases of solar cycle

The important parameter for semiannual variation of ionospheric ionization is the variation in atomic/molecular ratio, i.e. concentration of O/N_2 ratio. At solstice, there is circulation of meridional wind of about 25 m/s in middle and low latitudes from summer to winter hemisphere (Rishbeth et al., 2000). These winds carry nitrogen-rich air produced in summer hemisphere into lower latitudes by upwelling in higher latitudes, reducing O/N2 ratio. At equinox, there is no prevailing meridional circulation. The ratio O/N2 depends specially on the horizontal circulation, and its seasonal changes accompany the change in global thermospheric circulation between summer-to-winter pattern around the solstices to a symmetrical pattern at equinoxes. The six possible reasons of seasonal and semiannual variations in F_2 layer discussed by Rishbeth (1998) are: a) The compositional changes due to large-scale dynamical effects in the thermosphere b) Variations in the geomagnetic activities c) Energy of solar wind d) The inputs from lower atmospheric phenomena such as waves and tides e) change in atmospheric turbulence and f) Anisotropy of solar and EUV emission in solar latitude (Burkard, 1951).

In 2020, Ansari et al. found the minimum value of TEC in January and that becomes maximum in April then decreases in June-July and followed by increase in magnitude of second maximum in September-October and later decrease down till December at CHML and JMSM GRHI of year 2017. Referring Figure 8, our result of semiannual variation shows the minimum value of VTEC is found in January and that becomes maximum in March-April then decreases in June-July and followed by increase in magnitude of second maximum in October-November and later decreases down till December at GRHI of year from 2009 to 2018.

The asymmetry between the two equinoxes is due to geophysical parameters as magnetic indices related to geomagnetic activity (Triskova, 1989) and the IMF Bz the interplanetary component of magnetic field (Russell and McPherron, 1973). The equinoctial asymmetry observed in VTEC is explained by i) the axial hypothesis ii) the Russell McPherron (RM) effect and iii) the equinoctial hypothesis (ChamanLal, 1996; Shimeis et al., 2014).

Ouattara and Amory-Mazaudier (2012) made a statistical model of the F2 layer, at equatorial latitudes, based on data obtained during three sunspot cycles. This model shows the influence of the different type of geomagnetic activity defined by Legrand and Simon (1989) and the asymmetry of equinoxes due to the magnetic activity. The asymmetry between the two equinoctial peaks is also due to asymmetry of the thermospheric parameters that influence ionosphere as neutral wind and change in composition (Balan et al., 1998)

3.4 Solar cycle variation of TEC

Figure 9 shows the annual mean values of VTEC, solar flux index and sunspot number during the solar cycle from year 2008 to 2018. The black, blue, green and red color line represents VTEC variation on station KKN4, GRHI, JMSM and DLPA whereas pink and light green color line represents variation in SSN and solar flux index, respectively. The plot shows VTEC gradually begins to increase in 2009 and reaches a maximum in 2014. Then it begins to decrease till 2018 which agrees with the sunspot number and solar flux variation in the same plot. The figure shows that the maximum value of peak of ionization in 2014 about 37 TECU ~~tecu~~ in maximum phase of solar cycle and the minimum value in 2008 about 11 TECU ~~tecu~~ in the minimum phase of solar cycle. The observed VTEC variation corresponds to the amount of UV reach to the Earth.

Similarly, the solar flux increases from 2011 onward; the measured VTEC also exhibits highest magnitude for the year 2014. The maximum VTEC value shows a decreasing trend since year 2015 to 2018 at all the stations used for this study. It is observed from the graph that average annual VTEC shows better synchronization with SSN and solar flux index.

The patterns of the solar cycles play a major role in the solar variability: solar radiation and sunspot number and consequently influence the ionosphere. The solar cycle 24 is the smallest solar cycle since the spatial era (1957), in which peak is noticed in 2014, some few major solar flares were erupted from the Sun in February and October 2014 (Kane, 2002) so the maximum VTEC is noticed in February, October shown in Figure 8. Again from Figure 8, higher value of sunspot and solar flux was reported in February 2011 corresponding to X-class solar flare at which higher value of VTEC noted in station considered. Sharma et al. (2012) studied VTEC variation at Delhi lies near equatorial crest region during year 2007 to 2009 low solar activities and found TEC has a short-lived day minimum between 5:00-6:00 LT and gradual increase and reaches its peak value between 12:00 to 14:00 LT. The day minimum was found flat during most of the nighttime hours (22:00 to 06:00 LT). Their results show magnitude of daily maximum TEC decreases since 2007 to 2009 due to decrease in solar flux. They also found TEC seasonal behavior depends on the solar cycle and the largest daily TEC is observed during equinoctial month at Delhi. In 2020, Ghimire et al, studied diurnal variation of TEC at JMJG (Lamjung, Nepal) station for the year 2015 found the minimum in pre-dawn, a steady increase in the early morning followed by afternoon maximum then gradual decrease after sunset the similar pattern is also observed our study.

In African sector, Tariku (2015) observed from 2008 to 2009 and high 2012 to 2013 values of VTEC during the low and high solar activity phases. According to their finding, the diurnal VTEC values attained maximum in the time interval of 13:00 to 16:00 LT and the least values are mostly at around 06:00 LT. The similar result is noticed in all considered Nepalese GPS stations during the low solar active phases of solar cycle 24 in Nepal. The maximum diurnal variability in VTEC in 2014 is caused by solar active period confirmed by maximum sunspot number (SSN) and solar flux index (shown in Figure 2), VTEC greater in 2012 due to second maximum in SSN and solar flux and minimum VTEC in 2009 and 2017 supported by minimum SSN and solar flux which is confirmed by synchronization of VTEC with SSN and solar flux (Figure 9). In the ionosphere over Nepal the diurnal VTEC maximum occurs approximately between 12:00 to 14:00 LT. Similar to Delhi station in Nepal, the day minimum was found flat during most of the nighttime hours (22:00 to 06:00 LT). In general, the value of diurnal peak in VTEC is maximum during the spring equinoxes except in 2011 in which autumn VTEC is maximum. As the solar flux decreases from 2008 to 2009, the daily maximum VTEC values show a decreasing trend.

4 Conclusion

This paper investigates the diurnal, monthly, seasonal and solar cycle variations of VTEC at four mid low latitude stations: KKN4 (27.80° N, 85.27° E), GRHI (27.95° N, 82.49° E), JMSM (28.80° N, 83.74° E) and DLPA (28.98° N, 82.81° E) in Nepal.

The following conclusions are found:

- The shape of mean diurnal variation of VTEC depends on the solar cycle phases: flat ~~no~~ diurnal peak is observed during minimum and descending phases of the solar cycle whereas a Gaussian with different peak amplitude is noticed during ascending and maximum phases of the solar cycle.
- The study may reveal that diurnal TEC maximizes at around 11:00 LT to 14:00 LT, with minimum in the pre-dawn periods.
- Day to day variation in VTEC is significant in all the station. The maximum is noticed at KKN4 and minimum at DLPA.
- The mean diurnal profile in the year 2008, 2009, and 2010 ~~and 2017~~ exhibit wave like nature whereas the parabolic nature is observed in the year 2011, 2012, 2013, 2014, 2015, ~~and~~ 2016 and 2017.
- The week ionospheric activities characterized by lower TEC values during minimum and strong activities by higher value of VTEC during maximum phase ie VTEC has shown proper synchronization with SSN and solar flux.
- The monthly plot shows during sunrise time in summer the VTEC is linear whereas during the winter it is steep.

- Equinoctial asymmetry is not noticed in 2009, in 2011 autumn is more intense than spring and in 2014 and 2015 spring VTEC is greater than autumn.

- Equinoctial asymmetry in peak is noticed in spring (March, April) and autumn (September, October) in which higher is observed during spring.

-The equinoctial asymmetry is noticed in all the available stations due to difference in the F10.7cm for the two equinoxes.

-The spring-maximum is smaller than autumn-maximum mainly during years 2011, 2012, 2013 and also during year 2008 for one station, these years are years of minimum or increasing phase of the sunspot cycle.

-The VTEC in winter is greater than VTEC in summer ~~winter anomaly~~ is observed in all the available stations at the maximum of sunspot cycle 2014 and in one other station during the year 2011.

-During the year 2009 of the sunspot minimum the VTEC in winter is greater than VTEC in summer ~~winter anomaly~~ is not observed for all the stations. And there is no equinoctial asymmetry i.e. very weak (compare to the year of the maximum) except at JMSM.

-It seems that in Nepal for some years there is no semiannual variation, as we observe sometimes that the summer VTEC is larger than VTEC in the autumn. ~~It is probably a characteristic of Nepal.~~

The highest Himalayan mountains on earth in Nepal, are the source of landform waves that travel through the stratosphere and the lower thermosphere where they deposit their energy and give birth to secondary gravity waves that can affect VTEC. In our climatology study we analyze average behaviors that do not allow the study of these waves. Another study analyzing individually each day and using phase processing of GPS signals should be done in the future to analyze the impact of the Himalayas on VTEC and the impact of the low atmosphere on VTEC.

Acknowledgements

We acknowledge www.unavco.org,http://aiuws.unibe.ch/ionosphere (CODG), www.ngs.noaa.gov/CORS/Gpscal.shtml, and http://www.isgi.unistra.fr/, http://celestrack.com/GPS/almanar/Yuma/2017/, website: sidc.oma.be/silso/home and Omni data site http://omniweb.gsfc.nasa.gov/ for providing RINEX data for TEC, DCB file, Yuma file and data for solar wind parameters and geomagnetic indices for our calculations. The author would like to acknowledge Nepal Academy of Science and Technology (NAST), Nepal for proving PhD scholarship and ICTP, Italy for giving the opportunity to participate in a workshop on Space weather effects on GNSS operations at low latitudes.

References

Akala, A. O., Rabiu, A. B., Somoye, E. O., Oyeyemi E. O., Adeloye A. B. (2013). The Response of African equatorial GPS TEC to intense geomagnetic storms during the ascending phase of solar cycle 24, *Journal of Atmospheric and Solar-Terrestrial Physics,* **98**, 50–62, doi:10.1016/j.jastp.2013.02.006.

Ansari, K., Park, K. D., Panda, S. K. (2019). Empirical and orthogonal function analysis and modeling of ionospheric TEC over South Korean region, *ActaAstronautica*, **161**, 313-324, doi:10.1016/j.actaastro.2019.05.044.

Anderson, D., Fuller-Rowell, T. (1999). The ionosphere, Space environment topics SE-14, *Space Environment Center, Boulder, Report*.

Appleton, E. V. & Ingram, L. J. (1935). Magnetic Storms and Upper-Atmospheric Ionisation *Nature,***136**, 548–549.

Bagiya, M. S., Iyer, K. N., Joshi, H. P., Tsugawa, T., Ravindra, S., Sridharan, R., Pathan, B. M. (2011).Low-latitude ionospheric-thermospheric response to storm time electro dynamical coupling between high and low latitudes, *J. Geophys. Res.*, **116**, AO1303, doi:10.1029/2010JA015845.

Balan, N., Batista, I. S., Abdu, M. A., Macdougall, J., Bailey, G. J. (1998). Physical mechanism and statistics of occurrence of an additional layer in the equatorial ionosphere, *J. Geophys. Res.*, **103**(A12), 29,169–29,181, doi:10.1029/98JA02823.

Breit, G. ,Tuve, M. A. (1926). , A Test of the existence of the conducting layer, *Phys. Rev.*, **28**, 554–575.

Bremer, J. (2004). Investigations on long-term trends in the ionosphere with world-wide ionosonde observation, *Advances in Space Research***, 2**, 253–258, doi:10.5194/ars-2-253-2004.

Buonsanto, M. J. (1986). Possible effects of the changing Earth-Sun distance on the upper atmosphere, S. Pacific, *J. Nat. Sci*, **8**, 58-65.

Burkard, O. (1951). Die halbajahrige Periodic der F2-Schicht-Ionisation, *ArchivMeteorol. Bioklim, Wien*, **4**, 391-402

ChamanLal (1996). Seasonal trend of geomagnetic activity derived from solar-terrestrial geometry conforms an axial-equinoctial theory and reveals deficiency in planetary indices, *J. Atmos. Terr. Phys*., **58**, 1497-1506,doi: 10.1016/0021-9169(95)00182-4.

Chauhan V., Singh, O. P., Singh, B. (2011). Diurnal and seasonal variation of GPS-TEC during a low solar activity period as observed at a low latitude station Agra, *Indian Journal of Radio and Space Physics*, **40**, 26-36.

Cox, L. P., Evans, J. V. (1970).Seasonal variation of the O/N_2 ratio in the F_1 region, *J. Geophy. Res.*, **75**, 6271,doi:10.1029/JA075i051p06271.

D'ujanga, F. M., Mubiru, J., Twinamasiko, B. F., Basalirwa, C., Ssenyonga, T.J. (2012). Total Electron Content Variations in Equatorial Anomaly Region, *Advances in Space Research*, **50**, No. 4, 441–449, doi: 10.1016/j.asr.2012.05.005.

Dabas R.S., Lakshmi, D. R., Reddy, B. M. (1993). Solar activity dependence of ionospheric electron content and slab thickness using different solar indices, *Pure App. Geophys.*, **140**, 721-728.

Dashora, N., and Suresh, S. (2015). Characteristics of low-latitude TEC during solar cycles 23 and 24 using global ionospheric maps (GIMs) over Indian sector, *J. Geophys. Res. Space Physics*, **120**, 5176–5193, doi:10.1002/2014JA020559.

deAbreu, A. J., Fagundes, P.R., Gende, M., Bolaji, O. S., de Jesus, R., Brunini, C. (2014). Investigation of ionospheric response to two moderate geomagnetic storms using GPS-TEC measurements in the South American and African sectors during the ascending phase of solar cycle 24, *Advances in Space Research*, **53** (9), 1313–1328, doi:10.1016/j.asr.2014.02.011.

Galav, P., Dashora, N., Sharma, S., Pandey, R. (2010). Characterization of low latitude GPS-TEC during very low solar activity phase, *J. of Atmospheric and Solar –Terrestrial Physics*, **72**, 1309-1317, doi:10.10.1016/j.jastp.2010.09.017.

Ghimire,B.D, Chapagain, N.P., Basnet, V., Bhatt, K. and Khadka, B. (2020).Variation of Total Electron Content (TEC) in the quiet and disturbed days and their correlation with geomagnetic parameters of Lamjung Station in the year of 2015, *Bibechana*, **17**, 123-132 DOI: https://doi.org/10.3126/bibechana.v17i1.26249

Ghimire,B. D., Chapagain,N. P., Basnet,V., Bhatta,K. and Khadka,B. (2020).Variation of GPS-TEC Measurements of the Year 2014: A Comparative Study with IRI - 2016 Model. *Journal of Nepal Physical Society*, **6** (1), 90-96, DOI: http://doi.org/10.3126/jnphyssoc.v6i1.30555 90.

Gonzalez, W.D., Joselyn, J.A., Kamide. Y.,Kroehl, H.W., Rostoker, G, Tsurutani, B.T.andVasyliunas, V.M. (1994). What is geomagnetic storm? *J. Geophys.Res.*, **99**, 5771-5792, https://doi.org/10.1029/93JA02867

Guo, J., Li, W., Liu, X., Kong, Q., Zhao, C., Guo, B. (2015). Temporal-spatial variation of global GPS-derived total electron content, 1999-2013, *PloS ONE* **10**(7) e:0133378, doi:10.1371/journal.Pone 0133378.

Gupta, J. K. and Singh, L. (2001). Long term ionospheric electron content variations over Delhi, *Ann. Geophys*, **18**, 1635-1644, doi: 10.1007/s00585-001-1635-8.

Hofmann-Wellenhof, B., Lichtenegger H., Collins J. (1992).GPS: Theory and Practice, Springer Verlag/Wien, *ISBN 978-3-211-82364-6 and 978-3-7091-3298-5 (eBook).*

Huo, X. L., Yuan Y.B. ,Ou J.K., Zhang K.F., Bailey G.J. (2009). Monitoring the Global-Scale Winter Anomaly of Total Electron Contents Using GPS Data, *Earth Planets and Space*, **61**, 1019–1024, doi: 10.1186/BF03352952.

Jain, A.R. (1987). Reversal of EXB drift & post sunset enhancement of the ionospheric total electron content at equatorial latitudes, *Indian Journal of Radio and Space Physics*, **16**, 267-272.

Kane, R. P. (2002). Some implications using the group sunspot number reconstruction, *Solar Phys.*, **205**, 2, 383-401,doi:10.1023/A:1014296529097.

Khan A., Jin, S. (2018). Gravity wave activities in Tibet observed by Cosmic GPS radio, Geodesy and Geodynamics 9, 504-511, https://doi.org/10.1016/j.geog.2018.09.009

Kramkowsky, D., Kasprazak, W.T., Nier, A.O. (1968). Mass spectrometric studies of the composition of the lower thermosphere during summer 1967, *J. Geophys.Res*. **73**, 7291.

Legrand, J. P., Simon, P.A. (1989). Solar cycle and geomagnetic activity: A review for geophysicists. Part I. The contributions to geomagnetic activity of shock waves and of the solar wind, *Ann. Geophys*., **7**(6), 565-578

Martin, L. and Volkert, H. (2000), The Propagation of Mountain Waves into the Stratosphere: Quantitative Evaluation of Three-Dimensional Simulations, Journal of the Atmospheric Sciences Volume 57(18), DOI: https://doi.org/10.1175/1520-0469(2000)057<3090:TPOMWI>2.0.CO;2, 3090–3108.

Liu, G., Huang, W., Gong, J., Shem, H. (2013). Seasonal variability of GPS-VTEC and model during low solar activity period 2006-2007 near the equatorial ionization anomaly crest location in Chinese zone, *Advances in Space Research*, **51**, 366-376, doi: 10.1016/j.asr.2012.09.002.

Liu, L. B., Wan, W. X., Ning, B. Q., Zhang M. L. (2009). Climatology of the mean total electron content derived from GPS global ionospheric maps, *J. Geophys. Res.*, **114**: AO6308, doi: 10.1029/2009JA014244.

Liu, L. B., Chen, Y. D. (2009). Statistical analysis of solar activity variations of total electron content derived at Jet Propulsion Laboratory from GPS observations, *J. Geophys.Res.*, **114** :A10311, doi: 10.1029/2009JA014533.

Mansoori, A. A., Parvaiz A.K., Rafi A., Roshni A., Aslam A.M., Shivangi B., Bhupendra M., Purohit P.K., Gwal A.K. (2016). Evaluation of long term solar activity effects on GPS derived TEC, *Journal of Physics: Conference Series*, **759**, 012069, doi:10.1088/1742-6596/759/1/012069.

Natali, M. P., Meza A. (2011). Annual and Semiannual Variations of Vertical Total Electron Content during High Solar Activity Based on GPS Observations, *Ann. Geophys*., **29**, 865–873, doi: 10.5194/angeo-29-865-2011.

Ouattara, C., Amory-Mazaudier, C., Fleury, R., Lassudrie Duchesne, P., Vila, P., Petitdidier, M. (2009). West African equatorial ionospheric parameters climatology based Ouagadougou ionosonde station data from June 1966 to February 1998, *Ann. Geophys*., **27**, 2503-2514, doi: 10.5194/angeo-27-2503-2009.

Ouattara, F., Fleury R. (2011). Variability of CODG TEC and IRI 2001 Total Electron Content (TEC) during IHY Campaign Period (21 March to 16 April 2008) at Niamey under Different Geomagnetic Activity Conditions, *Scientific Research and Essays*, **6**, No. 17, 3609–3622.

Ouattara, F., Amory-Mazaudier, C. (2012).Statistical study of the equatorial F2 layer at Ouagadougou during solar cycles 20, 21, 22 using Legrand and Simon's classification of geomagnetic activity, *J.Space Weather Space Clim*., **2**, A19, doi:10.1051/swsc/20122019.

Parwani, M., Atulkar, R., Mukherjee, S., Purohit, P.K. (2019). Latitudinal variation of ionospheric TEC at northern hemispheric region, *Russian Journal of Earth Sciences*, **19**, ES1003, doi: 10.2205/2018ES000644.

Perevalova, N. P., Polyakova A.S., Zalizovski A.V. (2010). Diurnal Variation of the Total Electron Content under Quiet Helio-Geomagnetic Conditions, *Journal of Atmospheric and Solar-Terrestrial Physics*, **72**, 997–1007, doi: 10.1016/j.jastp.2010.05.014.

Prikryl, P., Jayachandran, P.T., Mushini S.C., Pokhotelov, D., MacDougall, J.W., Donovan E., Spanswick E., St-Maurice J.P. (2010). GPS TEC, scintillation and cycle slips observed at high latitudes during solar minimum, *AnnalesGeophysicae*, **28**, 1307-1316, doi: 10.5194/angeo-281307-2010.

Rama Rao P. V. S., Nru D., SriramaRao, M. (1980). Study of some low latitude ionospheric phenomena observed in TEC measurements at Waltair, India, *Proc. Satellite Beacon Symp.*, 57-65.

Rao, S.S., Chakraborty, M., Kumar, S., Singh, A.K. (2019a). Low-latitude ionospheric response from GPS, IRI and TIE-GCM TEC to Solar Cycle 24, *Astrophys Space Sci*, **364**:216, https://doi.org/10.1007/s10509-019-3701-2

Rao, S.S., Sharma, S., Pandey, R. (2019b).Study of solar flux dependency of the winter anomaly in GPS TEC, *GPS Solutions*, **23**(4) DOI: 10.1007/s10291-018-0795-x

Regmi, R.P. and Maharjan, S. (2015). Trapped mountain wave excitations over the Kathmandu valley, Nepal, Asia-Pacific Journal of Atmospheric Sciences volume 51, pages 303-309.

Regmi, R.P., Kitada, T., Dudha, J., Maharjan, S. (2017). Large-scale gravity over the middle hills of the Nepal Himalayas: implication for aircraft accidents, Journal of applied meteorology and climatology, pp 371-389, DOI: 10.1175/JAMC-D-160073.1

Rishbeth, *H.*, Garriott *O.K. (1969).* Introduction to Ionospheric Physics, *International Physics Series*, **14**, New York: Academic Press.

Rishbeth, H. (1998). How the thermospheric circulation affects the ionospheric F2- layer, *Solar-Terrestrial Physics*, **60**, 1385-1402, doi: 10.1016/S1364-6826(98)000062-5.

Rishbeth, H., Muller-Wodarg, I.C.F., Zou, L., Fuller-Rowell, Millward, G.H., Moffett, R. J., Idenden, D. W., Aylward, A. D. (2000). Annual and semiannual variations in the ionospheric F2-layer: II, physical discussion, *Ann.Geophysicae*, **18**, 945-956, doi: 10.1007/s00585-000-0945-6.

Rishbeth, H., Setty, C.S.G.K. (1961). The F-layer at sunrise, *J. Atmos. Terr. Phys*, **20**, 263-276, doi: 10.1016/0021-9169(61)90205-7.

Rothwell, P. (1963). Diffusion of ions between F layers at magnetic conjugate points, in Proc. International Conference on the Ionosphere, *Institute of Physics and Physical Society, London*, 217-221.

Russell C. T., McPherron R. L. (1973). Semiannual variation of geomagnetic activity, *J. Geophys. Res.*, **78**, 92-108, doi:10.1029/JA078i001p00092.

Sahai, Y., Becker-Guedes F., Fagundes P.R. (2007). Response of Nighttime Equatorial and Low Latitude F-Region to the Geomagnetic Storm of August 18, 2003, in the Brazilian Sector, *Advances in Space Research*, **39**, 1325–1334, doi: 10.1016/j.asr.2007.02.064

Sharma, K., Dabas, R.S., Ravindran, S. (2012). Study of total electron content over equatorial and low latitude ionosphere during extreme solar minimum, *Astrophs. Space Sci.*, doi 10.1007/s10509-012-1133-3.

Shimeis, A., Amory-Mazaudier, C., Fleury, R., Mahrous, A.M., Hassan, A. F. (2014). Transient variations of vertical total electron content over some African stations from 2002 to 2012, *Advances in Space Research*, **54**, 2159-2171, doi: 10.1016/j.asr.2014.07.038.

Tariku, Y.A. (2015). Patterns of GPS-TEC variation over low-latitude regions (African sector) during the deep solar minimum (2008 to 2009) and solar maximum (2012 to 2013) phases, *Earth Planet and Space*, **67**; 35, doi: 10.1186/s40623-015-0206-2.

Titheridge, J. F. (1972). The total electron content of the southern midlatitude ionosphere, 1965-1971, *J. Atmos. Terr. Phys.*, **35**, 981-1001, doi: 10.1016/0021-9169(73)90077-9.

Torr, M. R., Torr, D. G. (1973). The seasonal behavior of the F2-layer of the ionosphere, *J. Atmos. Terr. Phys*, **35**, 22-37, doi: 10.1016/0021-9169(73)90140-2.

Torre, A., Alexander, P., Llamedo, P., Hierro, R., Nava, B., Radicella, S., Schmidt, T. and Wickert, J. (2014). Wave activity at ionospheric heights above the Andes Mountains detected from FORMOSAT3/COSMIC GPS radio occultation data, Journal of Geophysical Research: Space Physics, 119(3):2046-2051.

Triskova, L. (1989). The vernal-autumn asymmetry in the seasonal variation of geomagnetic activity, *J. Atmos. Terr. Phys.*, **51**, 111-118, doi: 10.1016/0021-9169(89)90110-4.

Tyagi T.R., Das Gupta, A. (1990). Beacon satellite studies and modeling of total electron content of ionosphere, *Indian J. of Radio Space Phys*, 424-438.

Venkatesh, K., Fagundes P.R., de Jesus R., de Abreu A.J., Sumod S.G. (2014a). Assessment of IRI-2012 Profile Parameters by Comparison with the Ones Inferred Using NeQuick2, Ionosonde and FORMOSAT-1 Data during the High Solar Activity over Brazilian Equatorial and Low Latitude Sector, *Journal of Atmospheric and Solar-Terrestrial Physics*, **121**, 10–23, doi:10.1016/j.jastp.2014.09.014.

Venkatesh, K., Fagundes P.R., Seemala G.K., de Jesus R., Pillat V.G. (2014b). On the Performance of the IRI-2012 and NeQuick2 Models during the Increasing Phase of the Unusual 24th Solar Cycle in the Brazilian Equatorial and Low-Latitude Sectors, *J. Geophys. Res.*, **119**, 5087–5105, doi :10.1002/214JA019960.

Venkatesh, K., Fagundes P.R., Prasad D. S. V. V. D., DenardiniC.M. , de Abreu A.J., de Jesus R., Gende M. (2015). Day-to-Day Variability of Equatorial Electrojet and Its Role on the Day-to-Day Characteristics of the Equatorial Ionization Anomaly over the Indian and Brazilian Sectors, *J. Geophys. Res.*, **120**, 9117–9131, doi:10.1002/2015JA021307.

Walker, G. O., Ma J.H.K., Golton E. (1994). The Equatorial Ionospheric Anomaly in Electron Content from Solar Minimum to Solar Maximum for South East Asia, *AnnalesGeophysicae*, **12**, 195–209.

Wright, J.W. (1963). The F-region seasonal anomaly, *J. Geophys. Res.*, **68**, 4379-4381, doi: 10.1029/JZ068i014p04379.

Yonezawa, T. (1959). On the seasonal and non-seasonal annual variations and the semiannual variation in the noon and midnight densities of the F2 layer in middle latitudes II, J. Radio Res. Labs. Japan, **6**, 651-668.

Zakharenkova, I. E., Cherniak I.V., Krankowski A., Shagimuratov I.I. (2012). Analysis of Electron Content Variations over Japan during Solar Minimum: Observations and Modeling, *Advances in Space Research*, **52**, 1827–1836, doi: 10.1016/j.asr.2014.07.027.

Zhang, S.R., Holt, J.M., Anthony, P., Eyken, V., McCready, M., Amory-Mazaudier, C., Fucao, S., Sulzer, M., (2005).Ionospheric local model and climatology from long-term databases of multiple incoherent scatter radars, *Geophys. Res. Lett.*, **32,** L20102, doi.1029/2005GL023603

Zhao, B., Wan, W., Liu, L., Mao, T., Ren, Z., Wang, M., Christensen, A.B. (2007). Features of annual and semi-annual variations derived from the global ionospheric maps total electron content, *Annals Geophysicae*, **25**, 2513-2527, doi: 10.5194/angeo-25-2513-2007.

Zou, L., Rishbeth, H, Muller-Wodarg, I. C.F., Aylward, A.D., Millward, G.H., Fuller-Rowell, T.J., Idenden, D.W., Mofett, R.J. (2000).Annual and semiannual variations in the ionospheric F2-layer I Modeling, *Ann. Geophys.*, **18**, 944.

Zoundi, C., Ouattara F., Fleury R., Lassudrie-Duchesne P. (2012). Seasonal TEC Variability in West Africa Equatorial Anomaly Region, *European Journal of Scientific Research*, **77**, 303–313.

Tables Captions

Table 1.The selected GPS stations and their coordinates, the data of which are used in the study

Table 2. Classification of selected years according to the solar cycle phases

List of figures

Fig.1. A map of Nepal showing locations of GPS stations used in our study

Fig. 2 Display the variations of sunspot numbers and solar flux for the year 2008 to 2018.

Fig. 3a.Diurnal variation of vertical TEC in LT at KKN4 GPS station. The black, blue, light green, red and pink color line represent diurnal variation for the year 2009, 2012, 2014, 2016 and 2017 respectively.

Fig. 3b Diurnal variation of vertical TEC in UT at KKN4 GPS station. The first panel represents wave like mean diurnal curves of year 2008, 2009, 2010 ~~and 2017~~ and the second panel represents parabolic nature of mean diurnal curves of the year 2011, 2012, 2013, 2014, 2015, 2016 and 2017. The plots are arrange following on their diurnal profile.

Fig. 4.Monthlyvariation of vertical TEC in LT for each month of year 2014 at KKN4 station.

Fig. 5 (a), (b), (c) and (d). Two dimensional (2D) variation of vertical TEC according to UT at JMSM stations for one of the year of minimum (2009), ascending (2011), maximum (2014) and descending (2015) phases of solar cycle 24.

Fig. 6. Seasonal variability of VTEC during year 2008, 2009, 2011, 2014 and 2015 for KKN4, GRHI, JMSM and DLPA stations.

Fig. 7. Mean yearly seasonal variation of VTEC for year 2008 to 2017 at KKN4

Fig.8.Maximum VTEC variability at GRHI stations during minimum, increasing, maximum and decreasing phases of solar cycle 24

Fig. 9. Annual mean VTEC variability at KKN4, GRHI, JMSM and DLPA stations with SSN and solar flux during year 2008 -2018

Table 1

SN	ID	Locations	Geog. Lat.	Geog. Long.	Geom. Lat.	Geom. Long.	Dip Lat.	Local Time (LT)
1	KKN4	Kakani, Nepal	27.80° N	85.27° E	18.62°N	159.41° E	43.86	UT+5:45h
2	GRHI	Ghorahi, Nepal	27.95° N	82.49° E	18.94°N	156.82° E	44.25	UT+5:45h
3	JMSM	Jomsom, Nepal	28.80° N	83.74° E	19.71°N	158.06° E	45.31	UT+5:45h
4	DLPA	Dolpa, Nepal	28.98° N	82.81° E	19.94°N	157.21° E	46.03	UT+5:45h

Table 2.

Interval	Years	Solar cycle phases
I	2008, 2009	The minimum of solar cycle 24
II	2010, 2011	The increasing phase of solar cycle 24
II	2012, 2013, 2014	The maximum phase of solar cycle 24
IV	2015, 2016, 2017, 2018	The decreasing phase of solar cycle 24

Figure 1

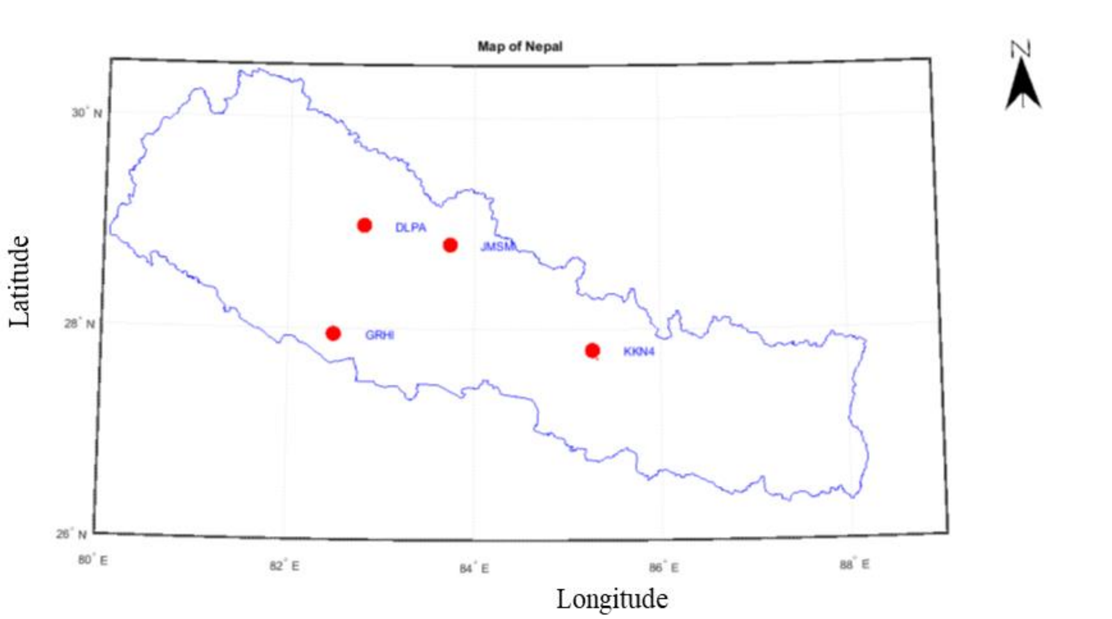

Map of Nepal
N
30° N
28° N
26° N
80° E
82° E
84° E
86° E
88° E
DLPA
JMSM
GRHI
KKN4
Latitude
Longitude

Figure 2

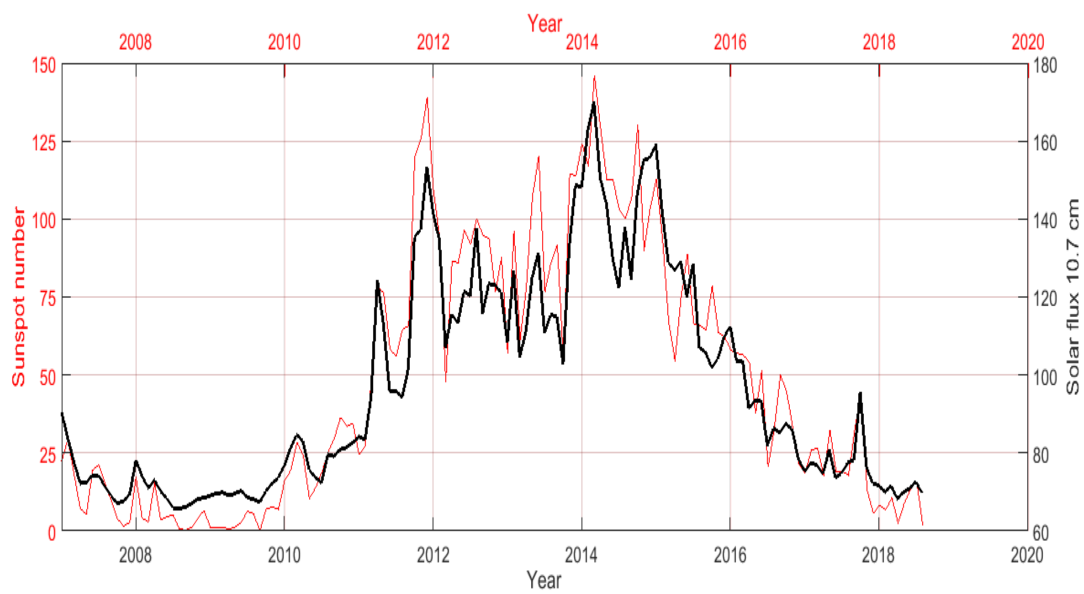
Year
2008
2010
2012
2014
2016
2018
2020
Sunspot number
150
125
100
75
50
25
0
Solar flux 10.7 cm
180
160
140
120
100
80
60
2008
2010
2012
2014
2016
2018
2020
Year

Figure 3a

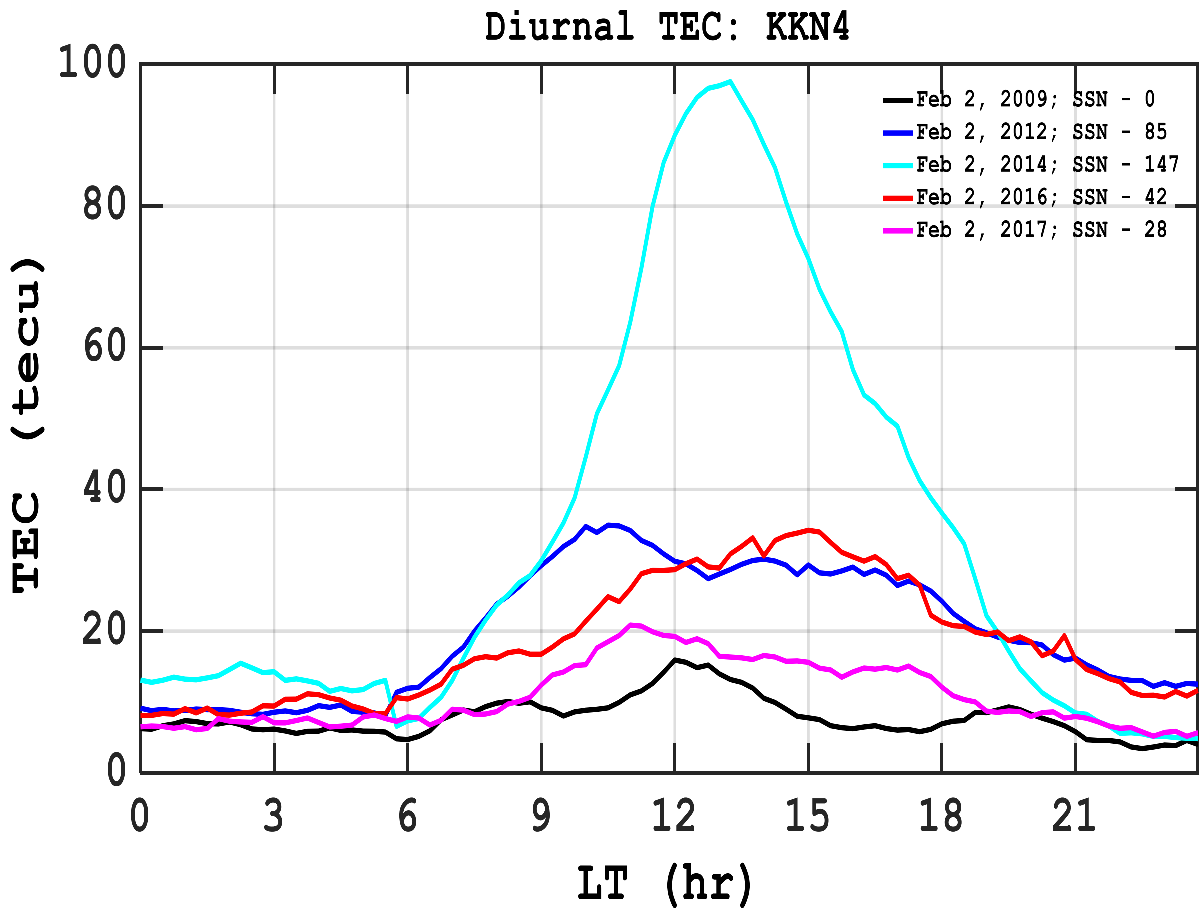
Diurnal TEC: KKN4
TEC (tecu)
LT (hr)
100
80
60
40
20
0
0
3
6
9
12
15
18
21
Feb 2, 2009; SSN - 0
Feb 2, 2012; SSN - 85
Feb 2, 2014; SSN - 147
Feb 2, 2016; SSN - 42
Feb 2, 2017; SSN - 28

Figure 3b

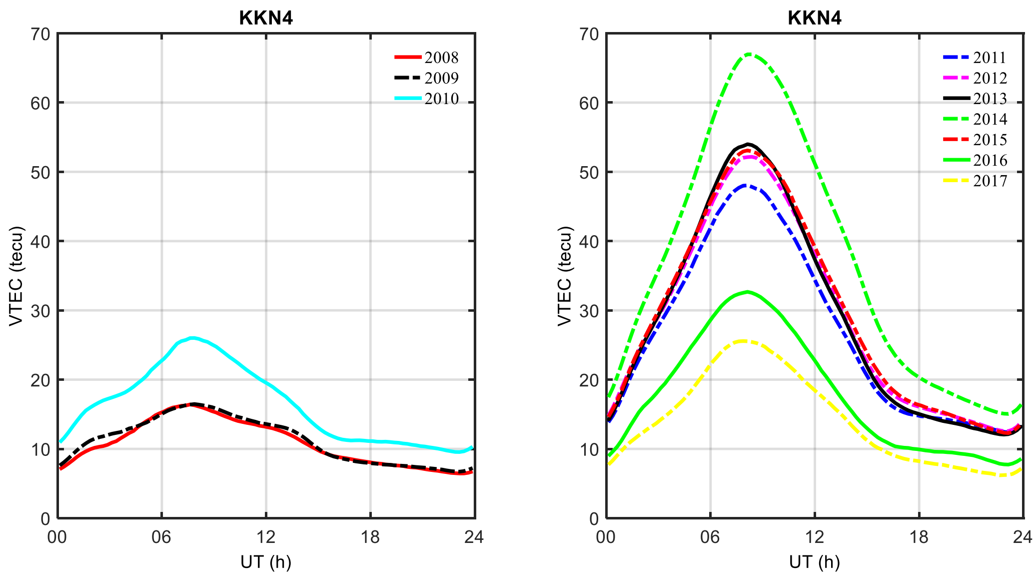
KKN4
VTEC (tecu)
UT (h)
2008
2009
2010
KKN4
VTEC (tecu)
UT (h)
2011
2012
2013
2014
2015
2016
2017

Figure 4

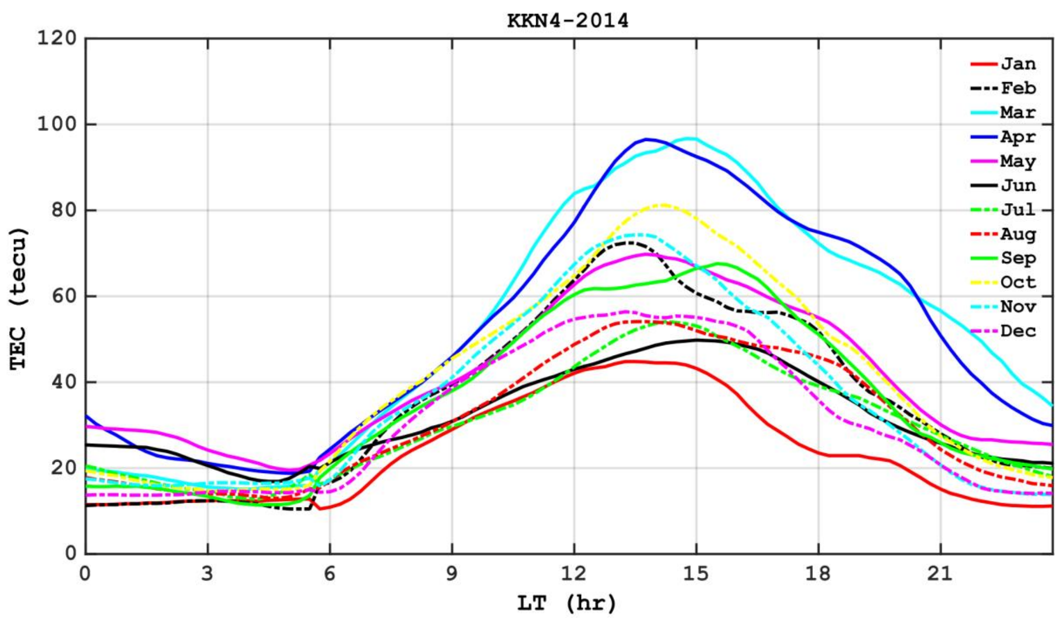
KKN4-2014
TEC (tecu)
LT (hr)
Jan
Feb
Mar
Apr
May
Jun
Jul
Aug
Sep
Oct
Nov
Dec
0
3
6
9
12
15
18
21
0
20
40
60
80
100
120

Figure 5a

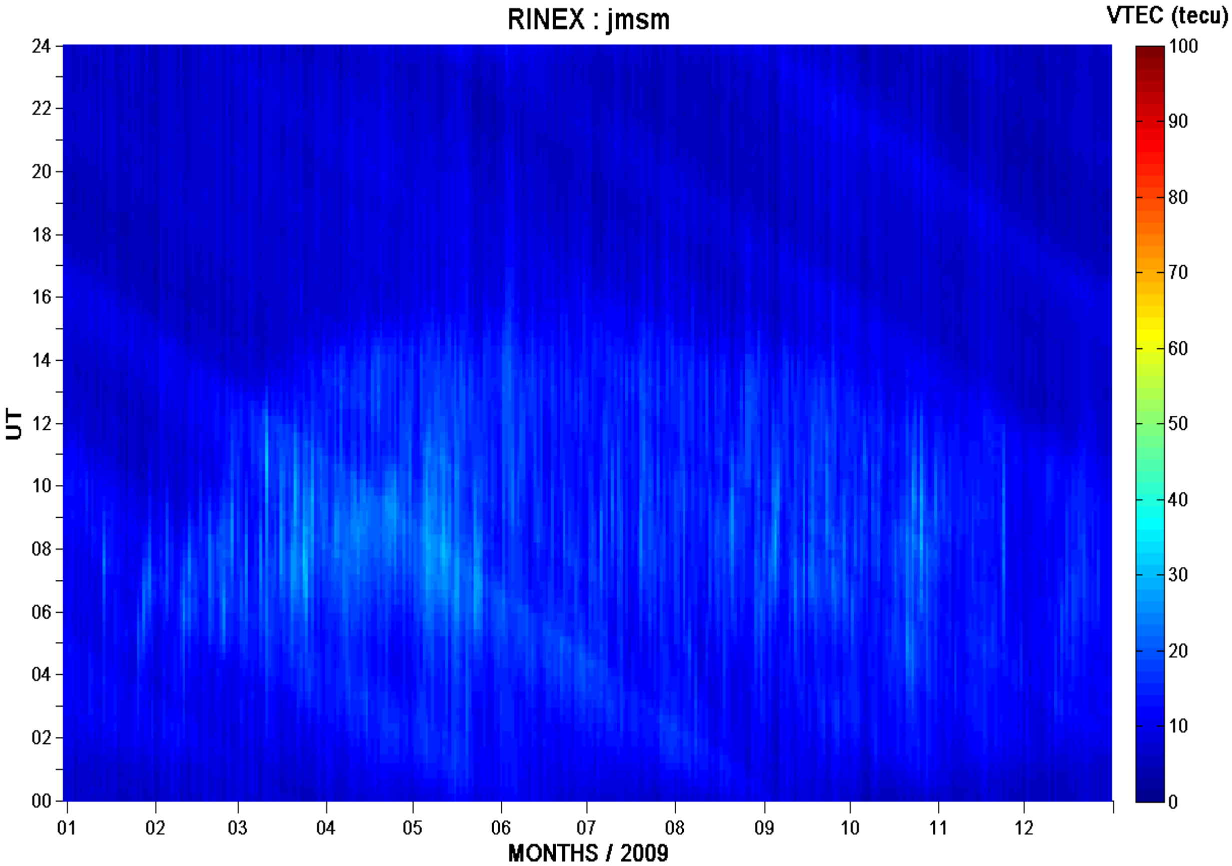

RINEX : jmsm
VTEC (tecu)
100
90
80
70
60
50
40
30
20
10
0
UT
24
22
20
18
16
14
12
10
08
06
04
02
00
01
02
03
04
05
06
07
08
09
10
11
12
MONTHS / 2009

Figure 5b

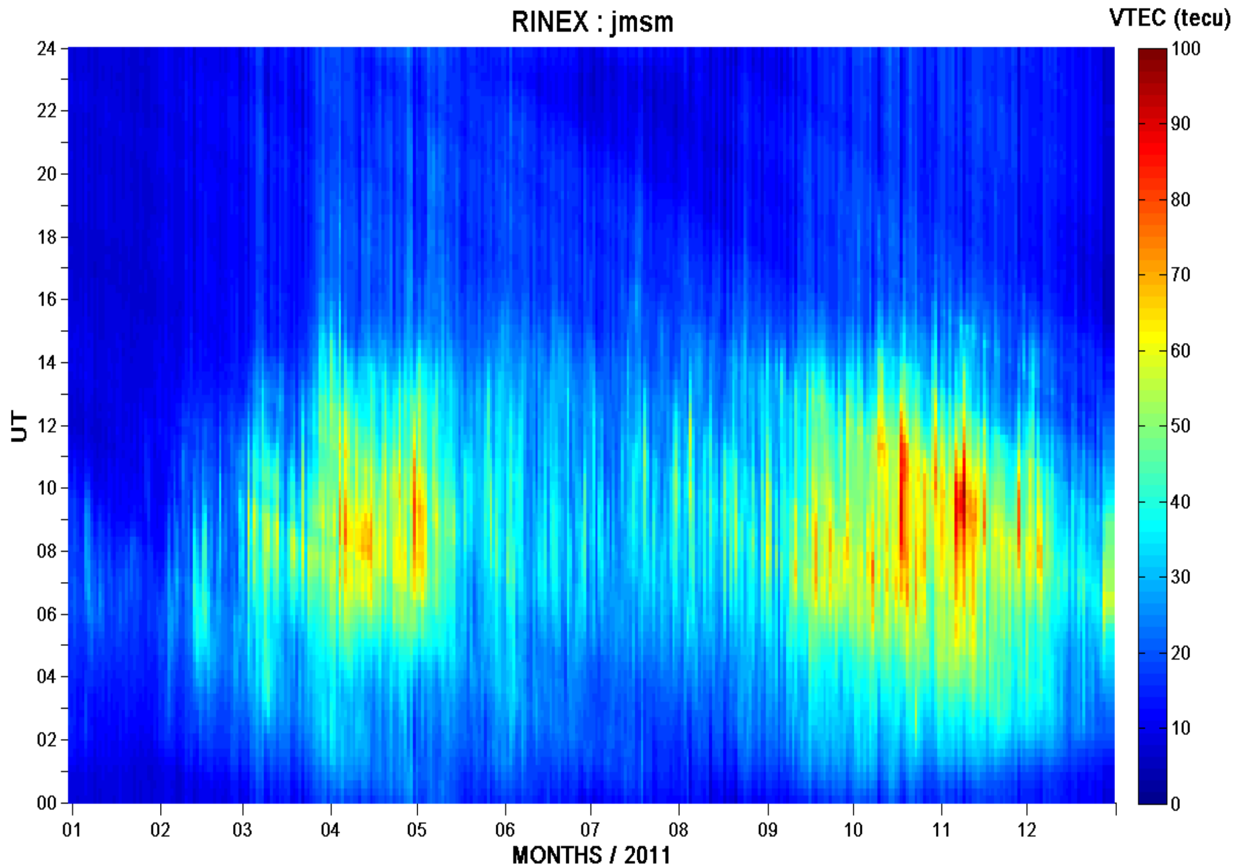
RINEX : jmsm
VTEC (tecu)
UT
MONTHS / 2011
00
02
04
06
08
10
12
14
16
18
20
22
24
01
02
03
04
05
06
07
08
09
10
11
12
0
10
20
30
40
50
60
70
80
90
100

Figure 5c

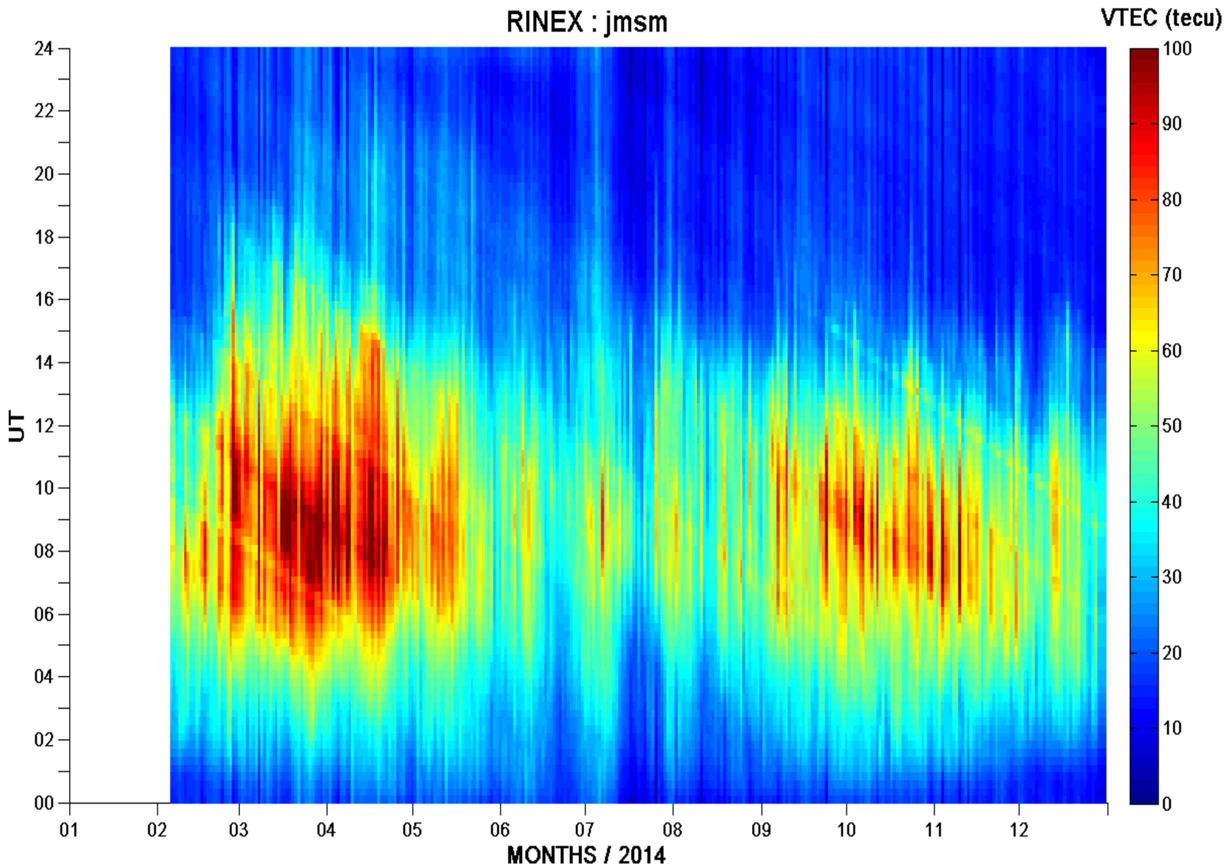
RINEX : jmsm
VTEC (tecu)
UT
MONTHS / 2014
24
22
20
18
16
14
12
10
08
06
04
02
00
01
02
03
04
05
06
07
08
09
10
11
12
100
90
80
70
60
50
40
30
20
10
0

Figure 5d

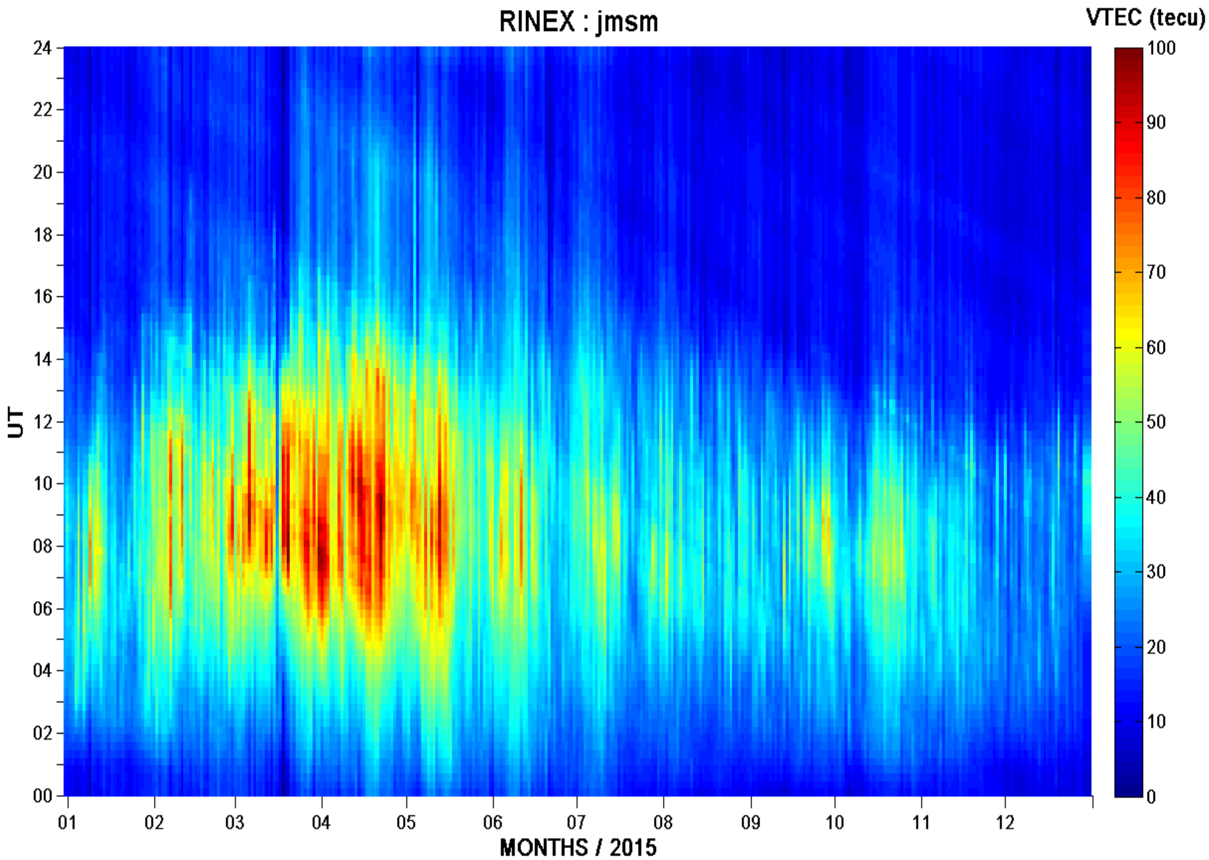
RINEX : jmsm
VTEC (tecu)
UT
MONTHS / 2015
24
22
20
18
16
14
12
10
08
06
04
02
00
01
02
03
04
05
06
07
08
09
10
11
12
100
90
80
70
60
50
40
30
20
10
0

Figure 6a

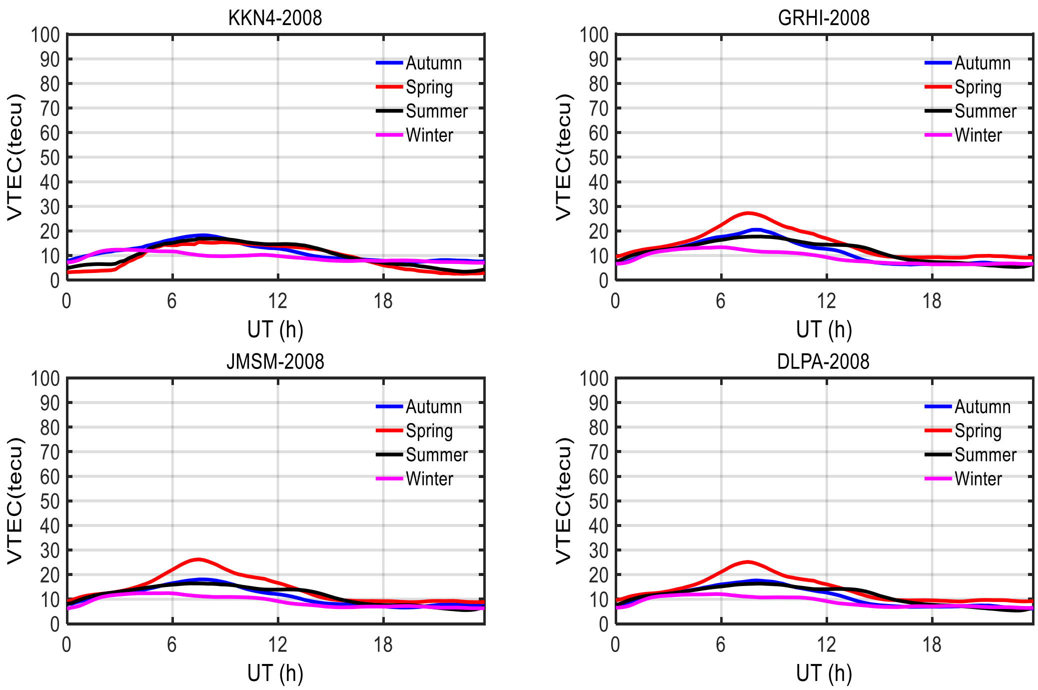
KKN4-2008
GRHI-2008
JMSM-2008
DLPA-2008
VTEC(tecu)
UT (h)
Autumn
Spring
Summer
Winter

Figure 6b

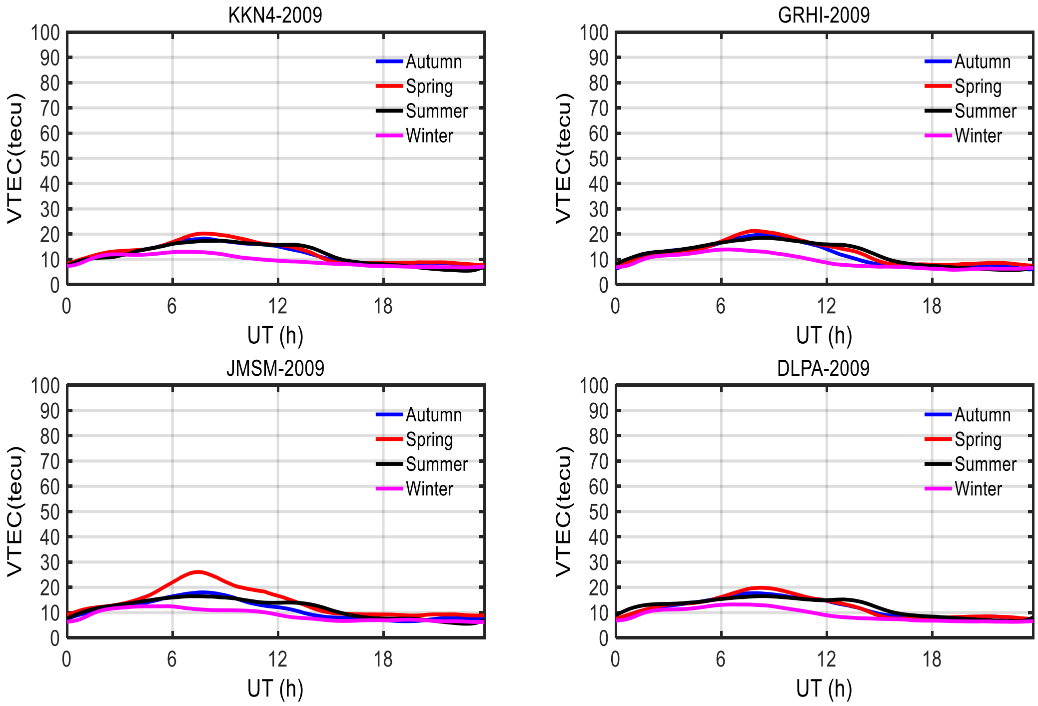
KKN4-2009
GRHI-2009
JMSM-2009
DLPA-2009
VTEC(tecu)
UT (h)
Autumn
Spring
Summer
Winter
0
10
20
30
40
50
60
70
80
90
100
0
6
12
18

Figure 6c

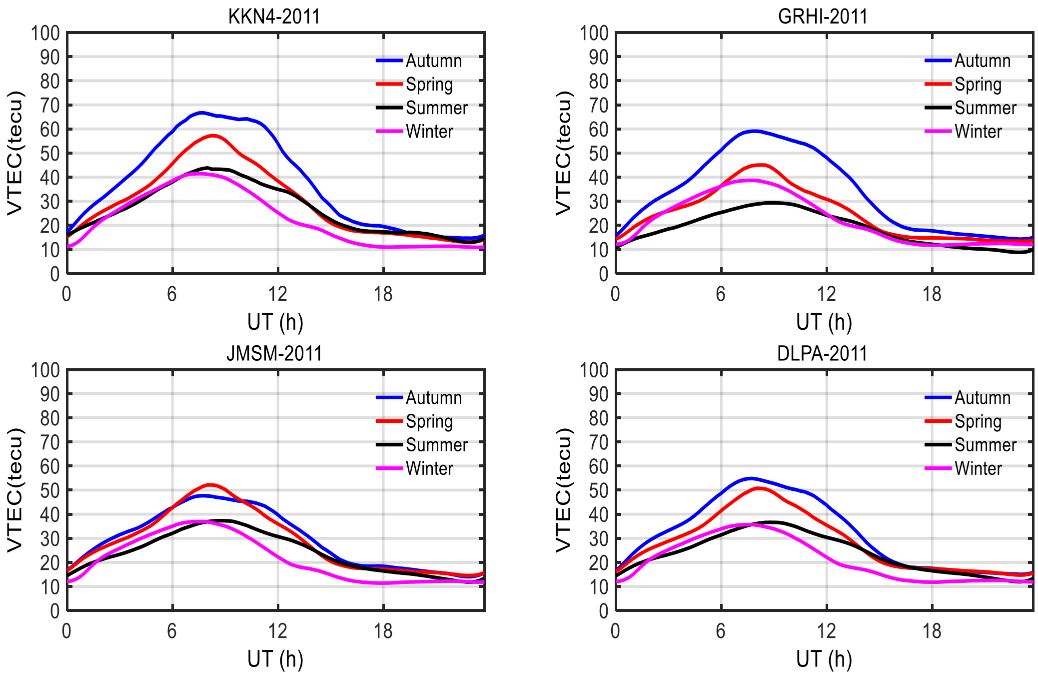
KKN4-2011
GRHI-2011
JMSM-2011
DLPA-2011
VTEC(tecu)
UT (h)
Autumn
Spring
Summer
Winter

Figure 6d

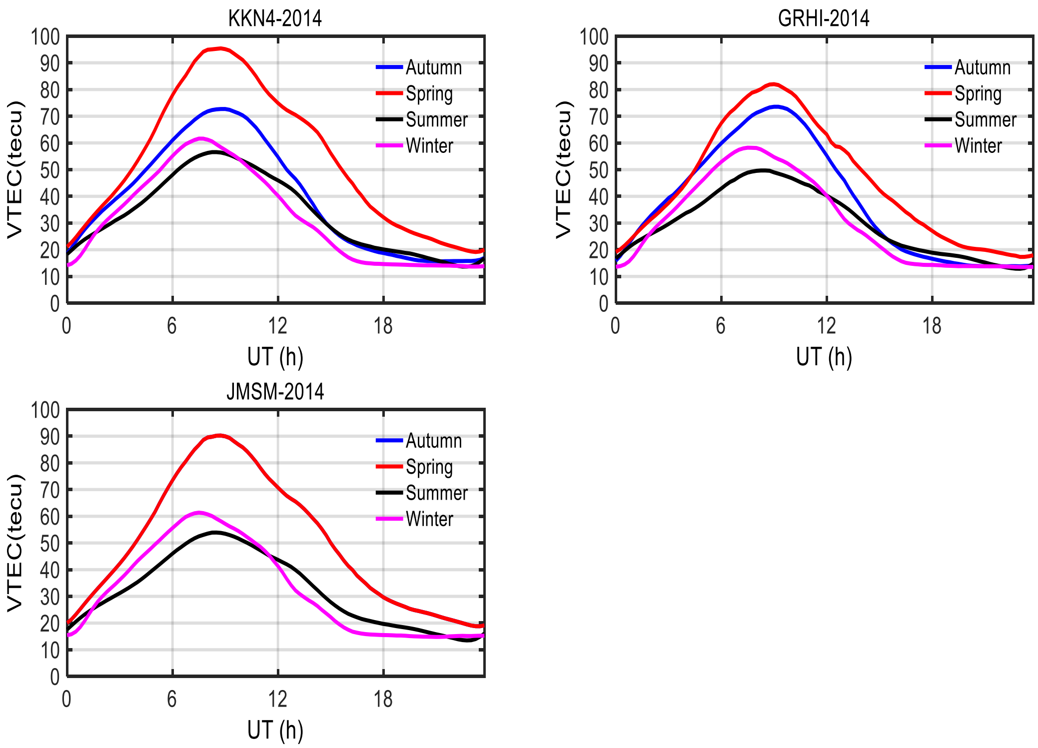
KKN4-2014
GRHI-2014
JMSM-2014
VTEC(tecu)
UT (h)
Autumn
Spring
Summer
Winter

Figure 6e

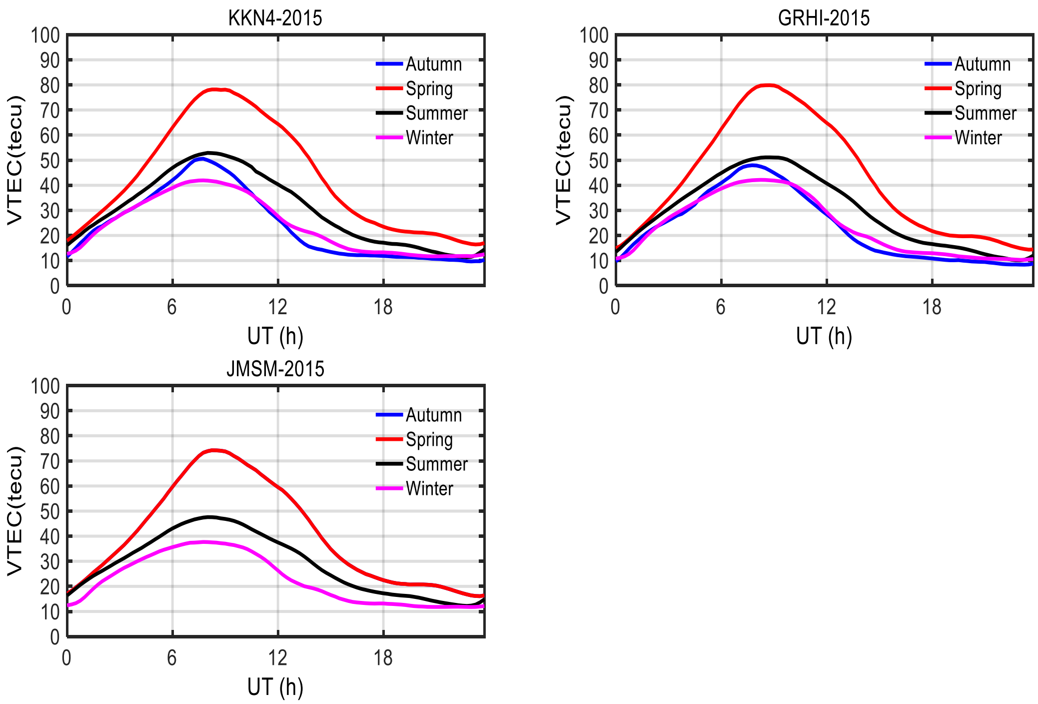
KKN4-2015
GRHI-2015
JMSM-2015
VTEC(tecu)
UT (h)
Autumn
Spring
Summer
Winter
0
10
20
30
40
50
60
70
80
90
100
6
12
18

Figure 7

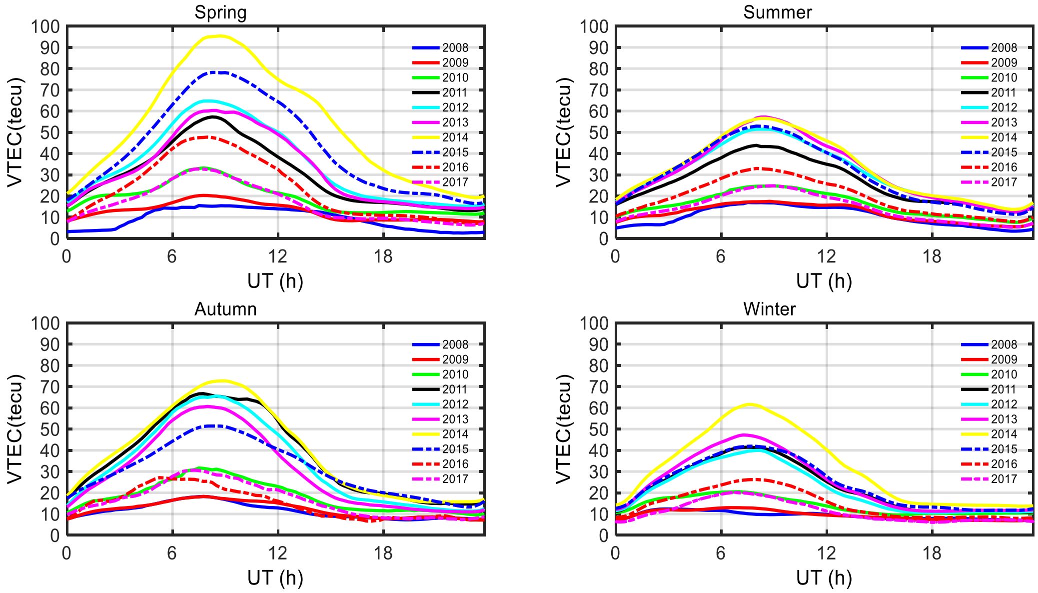
Spring
Summer
Autumn
Winter
VTEC(tecu)
UT (h)
2008
2009
2010
2011
2012
2013
2014
2015
2016
2017

Figure 8

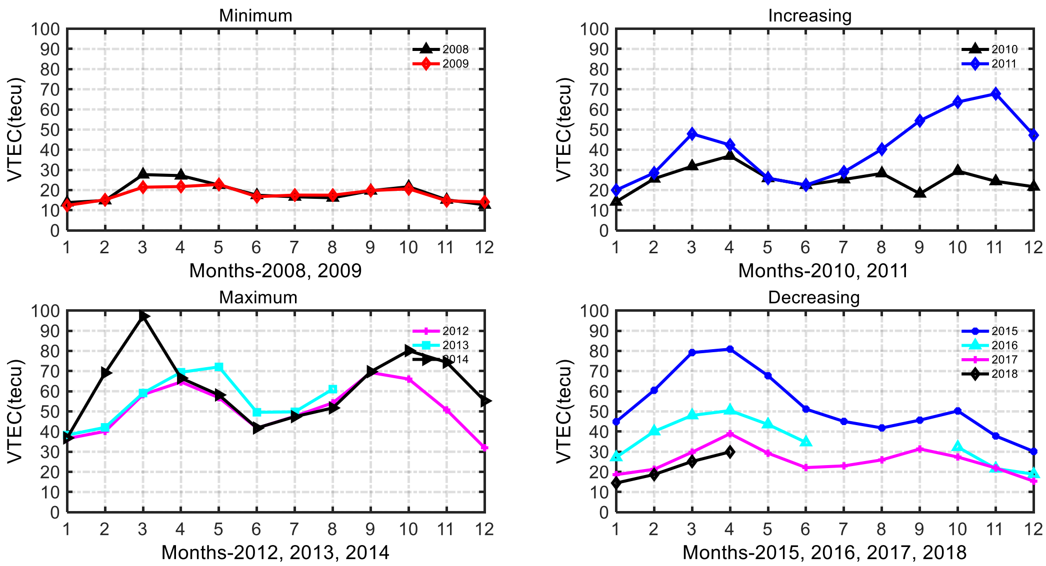

Minimum
VTEC(tecu)
2008
2009
Months-2008, 2009
Increasing
2010
2011
Months-2010, 2011
Maximum
2012
2013
2014
Months-2012, 2013, 2014
Decreasing
2015
2016
2017
2018
Months-2015, 2016, 2017, 2018

Figure 9

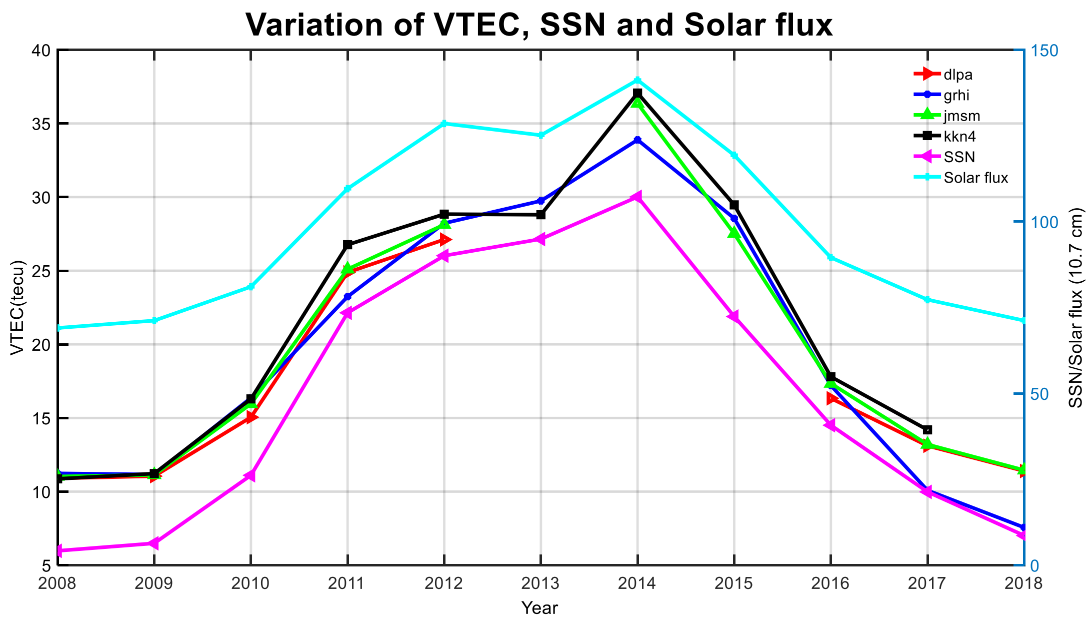
Variation of VTEC, SSN and Solar flux
VTEC(tecu)
SSN/Solar flux (10.7 cm)
Year
dlpa
grhi
jmsm
kkn4
SSN
Solar flux
40
35
30
25
20
15
10
5
150
100
50
0
2008
2009
2010
2011
2012
2013
2014
2015
2016
2017
2018